Peer-reviewed version available at *Biomolecules* **2017**, 7, , 44; doi:10.3390/biom7020044

Article

An Amyloidogenic Sequence at the N-Terminus of the Androgen Receptor Impacts Polyglutamine Aggregation

Emmanuel Oppong [1], Gunter Stier [2], Miriam Gaal [3], Rebecca Seeger [3], Melanie Stoeck [4], Marc-André Delsuc [1], Andrew C. B. Cato [3,*], Bruno Kieffer [1,*]

[1] Department of Integrative Structural Biology, Institut de Génétique et de Biologie Moléculaire et Cellulaire, INSERM, U964, CNRS, UMR-7104, Université de Strasbourg, 1 rue Laurent Fries, 67404 Illkirch–Graffenstaden, France; emmanopp@yahoo.com, Delsuc@igbmc.fr, kieffer@igbmc.fr

[2] Heidelberg University Biochemistry Center (BZH), INF 328, Heidelberg D-69120, Germany; gunter.stier@bzh.uni-heidelberg.de

[3] Institute of Toxicology and Genetics, Karlsruhe Institute of Technology, Hermann-von-Helmholtz-Platz 1, 76344 Eggenstein-Leopoldshafen, Germany; miriamgaal@icloud.com, rebecca.seeger@kit.edu, andrew.cato@kit.edu

[4] Institute for Photon Science and Synchrotron Radiation, Karlsruhe Institute of Technology, Hermann-von-Helmholtz-Platz 1, 76344 Eggenstein-Leopoldshafen, Germany; melanie.stoeck@gmx.de

* Correspondence: andrew.cato@kit.edu Tel: +49 721 608 22146 kieffer@igbmc.fr ; Tel.: +33 3 68 85 47 22

Abstract: The human androgen receptor (AR) is a ligand inducible transcription factor harboring an amino terminal domain (AR-NTD) hosting the ligand independent activation function. AR-NTD is intrinsically disordered and display aggregation properties conferred by the presence of a poly-glutamine (polyQ) sequence of 22 residues. The length of the polyQ sequence, as well as the presence of adjacent sequence motifs modulate this aggregation property. AR-NTD contains also a conserved sequence motif KELCKAVSVSM that displays an intrinsic property to form amyloid fibrils under mild oxidative conditions of its conserved cysteine residue. As peptide sequences with intrinsic ability to oligomerize are reported to have an impact on the aggregation of polyQ tract, we determined the effect of the KELCKAVSVSM on the polyQ stretch in the context of the AR NTD, using Atomic Force Microscopy (AFM). Here, we present evidence for a crosstalk between the amyloidogenic properties of the KELCKAVSVSM motif and the polyQ stretch at the AR NTD.

Keywords: amyloid peptides; androgen receptor; nuclear receptor; aggregation; atomic force microscopy

1. Introduction

The human androgen receptor (AR) is a ligand inducible transcription factor and a member of the nuclear receptor family that includes the glucocorticoid receptor (GR), mineralocorticoid receptor (MR), estrogen receptor (ER) and progesterone receptor (PR). This protein consists of 919 amino acids and is organized into an amino terminal domain (NTD, 1-559), a DNA binding domain (DBD, 559-624), a hinge region (HR, 624-706) and a carboxy-terminal ligand binding domain (LBD, 706-919). The LBD and DBD display conserved and well characterized three-dimensional folds [1-3]. In contrast, the NTD is described as an intrinsically disordered region, a feature that hampers the elucidation of simple sequence-function relationship [4]. Notwithstanding its lack of a defined fold, several features of the transcriptional activity of AR are attributed to the NTD where several short peptide motifs are involved in the modulation of full-length AR transcriptional activity [5,6]. AR NTD sequence features also several low complexity regions, such as homopolymer stretches of glutamines (polyQ), glycines (polyG) or prolines (polyP) whose biological role remains unknown. Extension of the polyQ sequence above 40 residues is however associated with the neurodegenerative disease spinal and bulbar muscular atrophy (SBMA) [7] while shortening of this

homopolymer below 20 residues may be responsible for increased prostate cancer risk [8]. A correlation between the length of the polyQ sequence, the morphology of AR oligomers and AR-mediated neurotoxicity has been established [9]. Atomic Force Microscopy (AFM) analyses of full-length AR showed that AR with 65 glutamine residues (ARQ65) forms fibrillar oligomers which are toxic in neuronal cells while AR with 22 glutamines forms non-toxic annular oligomers.

Protein oligomerization mediated by polyQ stretches are often modulated by the presence of adjacent domains or short sequence motifs that can either act as enhancers or repressors of the oligomerisation process. Recently, biophysical studies showed that a leucine-rich motif located at the N-terminal edge of AR polyQ region has an inhibitory effect on polyQ mediated AR aggregation [10]. Other examples where the aggregation of a polyQ stretch is enhanced by its flanking regions can be found in Huntington, Ataxin 3 and Ataxin 1 where the 17 amino acids N-terminal sequence of Huntington, the Josephin domain and the AXH domain trigger a first step of aggregation of polyQ tracts containing proteins [11-13]. Although these sequences are non-polyQ, they have an intrinsic property to aggregate and this impacts on the aggregation properties of their adjacent PolyQ counterparts.

We have recently shown that synthetic KELCKAVSVSM peptides derived from the AR NTD has an intrinsic property to form amyloid fibril under mild oxidative conditions [14]. It is therefore likely that this sequence would have an effect on aggregation of the polyQ track at the AR NTD. In the present communication we present evidence for a crosstalk between the amyloidogenic properties of the KELCKAVSVSM motif and the polyQ stretch at the AR NTD.

2. Results

2.1 Amyloidogenic properties of KELCKAVSVSM peptides expressed as SUMO fusion proteins

We have previously reported amyloidogenic properties of a conserved sequence from the central region of AR-NTD [14]. These experiments, conducted with peptides of various lengths, identified the sequence KELCKAVSVSM as the minimal motif for the formation of amyloid fibers upon addition of 10% DMSO. To determine whether the amyloidogenic property of this sequence is retained in a larger peptide, in the context of a fusion protein, we fused the peptide to a SUMO protein and expressed it in E coli [21]. After affinity purification of the bacterial cell lysates on nickel agarose resins, a major product with the expected mass of the HisSUMO-peptide fusion protein of 15.819 kDa was identified on a SDS-PAGE gel (Figure 1A, lane 5). In addition, a distinct protein with a higher molecular weight was also identified (Figure1A, see asterisks).

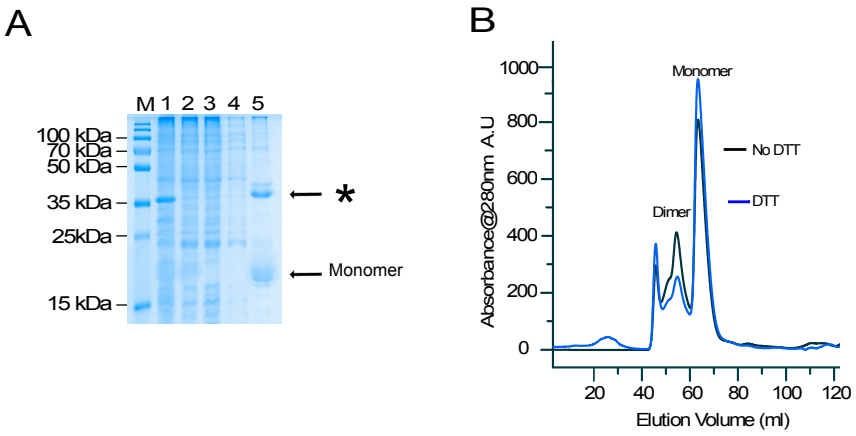

Figure 1. (A) Non-reducing SDS-PAGE analysis of the affinity purification of the HisSUMO fusion peptide fusion expressed showing the total extract (lane 1), the soluble extract (lane 2), the flow-through fraction from the nickel NTA column (lane 3), the wash fraction (lane 4) and the elution fraction (lane 5). (B) Size exclusion chromatography analysis of HisSUMO peptide from LB medium in buffer with DTT (black), no DTT (red).

To determine the identity of the additional product, the HisSUMO-peptide fusion protein was subjected to size exclusion chromatography (SEC) with or without the addition of the reducing agent, dithiothreitol (DTT) (Figure 1B). Both conditions led to similar SEC profiles with a major sharp and symmetrical peak eluting at 64 ml, indicative of a pure and homogenous protein. Another peak with a higher molecular weight protein, eluting from 55 ml to 60 ml was also identified, although this fraction was significantly decreased when DTT was added to the elution buffer (Figure 1B). Mass spectrometry analysis unambiguously identified the lower and higher molecular weight fractions to be SUMO-KELCKAVSVSM fusion protein and its covalent dimer, respectively. Since SUMO has no cysteine in its sequence, the observed dimerization may be attributed to the formation of an inter-molecular disulfide bridge mediated by the cysteine within the peptide.

We have previously shown that the KELCKAVSVSM forms fibrils under mild oxidation conditions [14]. We therefore determined whether the SUMO-KELCKAVSVSM fusion proteins (either in the monomer or dimer form) would form amyloid fibers but this failed after repeated attempts. Since the SUMO tag may mask the formation of the fibrils, we determined the accessibility of the peptide in the context of the fusion protein. We compared the ^{1}H-^{15}N heteronuclear single quantum coherence (HQSC) spectra with or without the SUMO tag to determine the disordered state of the peptide within the fusion protein. The ^{1}H-^{15}N HQSC correlations corresponding to the peptide alone (without the tag) was completely superimposable on the correlations present in the HisSUMO-peptide fusion protein in the spectral region corresponding to amide protons from disordered residues (8.0 to 8.4 ppm, see Figure 2). This finding highlights the lack of interactions between the SUMO fusion protein and the peptide, suggesting that the inhibitory effect of the SUMO protein on the fibrillation process is not related to a lack of peptide accessibility.

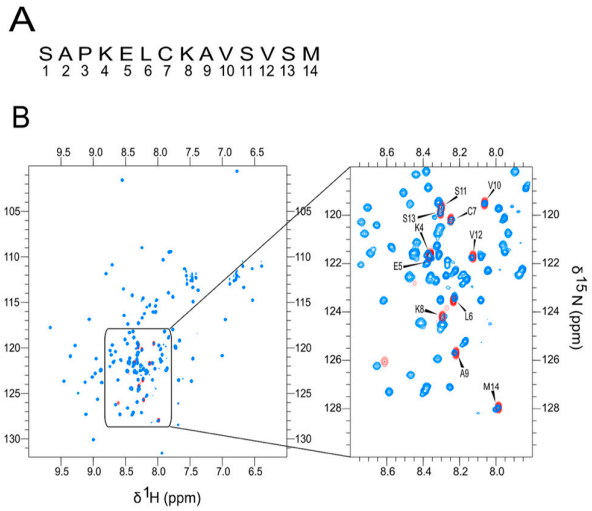

Figure 2. An overlay of the amide region of the ^{1}H-^{15}N HSQC spectrum of the HisSUMO-peptide fusion (blue) and the cleaved peptide (red).

We then cleaved the SUMO tag, HPLC purified the cleaved peptide and added 10 % DMSO to the sample. DMSO is a mild but specific oxidant of cysteines [22] that triggers the formation of covalent dimers, which could be followed by self-association of the dimers into amyloid fibers. Proton 1D NMR spectra recorded every half hour for 24 h after DMSO addition showed the gradual time-dependent disappearance of all the resonances corresponding to the formation of large sedimenting oligomers indicative of amyloid fibril formation (Figure 3A). This was confirmed by transmission electron microscopy (TEM) analysis of the pelleted material in the NMR tube after the 24 h incubation. The resulting images displayed numerous fibrils with a large distribution of lengths but similar widths in agreement with our previous report [14].

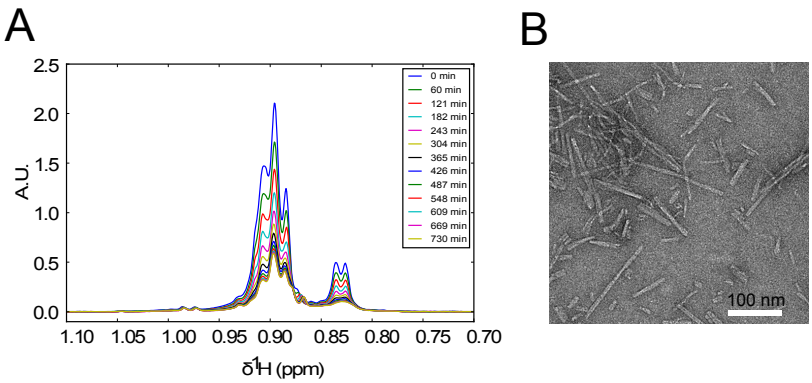

Figure 3. (A) Time dependence of the methyl region of proton NMR spectra of the recombinant peptide recorded shortly after addition of 10% DMSO at 298 K. The observed decrease of signal intensity is due to the formation of amyloid fibers that are not observed in the spectrum. (B) A TEM image of the NMR sample 24 h after addition of 10% DMSO showing the presence of fibrils of variable length.

2.2 The KELCKAVSVSM sequence modulates the polyQ oligomerisation properties of large AR-NTD fragments.

As peptide sequences with intrinsic ability to oligomerize are reported to have an impact on the aggregation of polyQ tracts [23], we determined the effect of the KELCKAVSVSM on the polyQ stretch in the context of the AR NTD. We expressed the KELCKAVSVSM (with or without a cysteine to serine mutation) and polyQ stretches of 22 or 45. As controls, we also expressed sequences covering only the KELCKAVSVSM with or without the cysteine mutation or only polyQ stretches of 22 or 45 (Figure 4A). All the peptides were first expressed as GST fusion proteins and their conformation was determined by atomic force microscopy AFM.

Preprints (www.preprints.org) | NOT PEER-REVIEWED | Posted: 16 May 2017 doi:10.20944/preprints201705.0126.v1

Peer-reviewed version available at Biomolecules 2017, 7, , 44; doi:10.3390/biom7020044

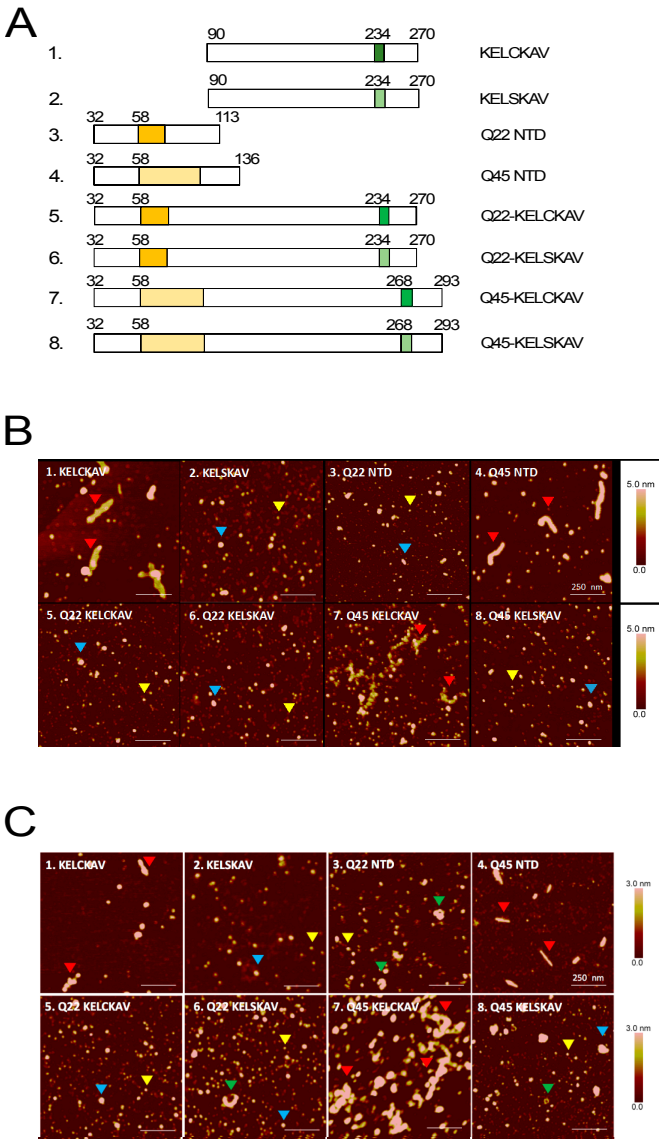

Figure 4. Schematic representation of AR NTD peptides covering the polyQ stretch (Q22 and Q45) stretch and the KELCKAVSVSM sequence (in dark green) or with the cysteine mutation KEL**S**KAVSVSM (light green). **B.** GST tagged AR NTD or **C.** untagged AR NTD proteins were incubated for 18 h at 37 °C to initiate the aggregation process before spotting on mica for AFM measurements. Blue and yellow arrow heads refer to smaller and larger globular oligomers (SGOs and LGOs); green arrow heads refer to annular oligomers and red arrow heads to fibrillar oligomers.

These analyses revealed the formation of smaller and larger globular oligomers (SGOs and LGOs) with diameter of 9-24 and 35-68 nm as we have previously published [9] (yellow and blue respectively arrow heads (Figure 4B). Fragments containing either an expansion of the polyQ stretch to 45 (Q45) or the KELCKAVSVSM sequence formed fibrillar oligomers (Figure 4B, red arrow heads panels 1, 4) and fibrils were also observed when both sequences were present (panel 7). However, fibrillar oligomers were undetectable when the cysteine residue was changed into a serine (Figure 4A and Figure 4B panel 2 and 8).

To rule out the possibility of the GST tag affecting the fibrillization process, we cloned the DNA sequences coding for these peptides into a pET-Gb1a vector and cleaved off the GB1 tag with a TEV protease after protein production releasing the untagged AR NTD fragments. Analysis of these untagged fragments by AFM produced results similar to those obtained with the tagged peptides

(compare Figures 4C with 4B). The only difference was a slight variation in the sizes and shapes of the fibrillar oligomers. The fibrillar oligomers in the GST tagged fragments were thicker than their untagged counterparts and additionally annular structures showed up particularly in samples containing untagged polyQ22. (Figure 4C panels 3 and 6; arrow heads). The Q45-KELCKAV fibrils formed by the fragment containing both the polyQ amplification and the KELCKAVSVSM were somewhat different. They consisted of bundles of fibrillar aggregates (Figures 4 B and 4C panel 7) but these were no longer visible when the cysteine in KELCKAVSVSM was substituted by a serine (Figures 4B and 4C panel 8). No significant change in the structure of oligomers was observed in fragments containing polyQ22 and KELCKAVSVSM with or without a cysteine to serine mutation (Figures 4B and 4C panels 5 and 6). Thus the major change in morphology of the fibrillar oligomers in the AR-NTD fragments following the cysteine to serine exchange in the KELCKAVSVSM sequence suggests that this motif contributes to the fibril formation of larger fragments containing amplified polyQ (poly 45) stretch.

3. Discussion

There are nine proteins that contain polyQ stretches which when amplified promote protein aggregation and are neurotoxic. This phenomenon has generated a family of polyQ disorders such as Huntington's disease, several spinocerebellar ataxias or the X-linked spinal and bulbar muscular atrophy (SMBA). The aggregation properties of the polyQ sequences of these proteins is controlled by many factors among which are intrinsic factors such their length but also the presence of adjacent sequence motifs.

The role of flanking sequence motifs as modulators of polyQ mediated protein aggregation is currently emerging as a common mechanism for aggregation. So far there are three well-known examples of this. A 17 amino acid N-terminal domain (N17) that flank the polyQ tract of huntingtin is known to have self-association properties that promote polyQ aggregation of Huntington [24],[25]. The Josephin domain (JD) of Ataxin 3 displays a fibrillogenic behavior that affects the aggregation of Ataxin 3 [26] [27] and a further example is the ataxin-1/HBP1 (AXH) domain of ataxin-1 that also controls polyQ-mediated aggregation of Ataxin 1. So far no such domain has been identified in the remaining 6 out of the 9 polyQ proteins. We have previously identified an evolutionary conserved sequence motif KELCKAVSVSM at the N-terminus of the AR that formed fibrillar aggregates but not when the cysteine it contains was converted into a serine. The aggregates formed by this sequence bound thioflavin T which is a feature shared by amyloid fibers and polyQ aggregates, although it is in itself a non-polyQ peptide. A possibility therefore exists that this sequence would contribute as a nucleation center to the aggregation properties of the polyQ stretch that is located approximately 200 amino acids at its N-terminal sequence.

In the present report we show that although it formed aggregates, when tagged with a SUMO protein, the KELCKAVSVSM peptide formed only dimers, but no further high molecular weight species. When the SUMO tag was cleaved, the peptide was able to undergo further aggregation to form fibrils. Furthermore when the length of the peptide was extended by over 200 amino acids to encompass the expanded polyQ stretch (polyQ45) of the AR, the ability to form fibrils was maintained. This shows that the sequence composition that surrounds the KELCKAVSVSM peptide determines whether its fibrillar aggregation properties could be impacted to a larger fragment or not. Other sequence motifs, such as a leucine-rich motif located at the N-terminal edge of AR polyQ region have been shown to have inhibitory effect on polyQ mediated AR aggregation [10]. It therefore appears that an interplay of positive and negative cis-regulatory elements control the aggregation properties of the polyQ containing proteins (Figure 5).

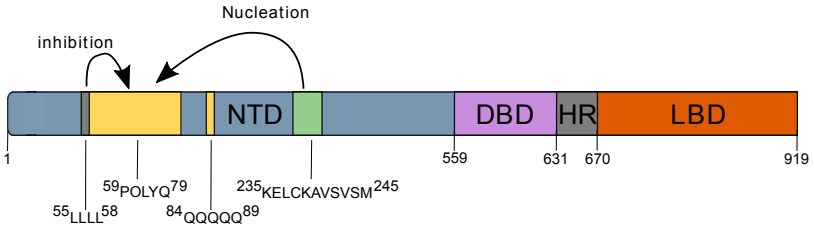

Figure 5. Schematic view of the different possible interactions in Androgen Receptor with an impact on AR aggregation.

We could also show in our study that when the polyQ stretch in the surrounding sequences of the KELCKAVSVSM is 22 rather than 45, the fibrillogenic properties of the KELCKAVSVSM is abrogated. It is therefore not only the KELCKAVSVSM motif, the polyQ stretch and the amino acid composition that determine the state of aggregation, but probably the distance between these sequences is equally important. Collectively our results demonstrate the existence of a crosstalk between the elements at the AR N-terminus in the control of polyQ stretch aggregation. The highly conserved nature of the KELCKAVSVSM motif suggests that its effect on the AR-NTD aggregation may be part of a complex regulatory mechanism whose details remain to be elucidated.

4. Materials and Methods

4.1 Cloning, protein expression and purification

AR N-terminal domain (NTD) constructs: Fragments encompassing 30 amino acids on each side preceding and following the polyQ stretches of 22 and 45 from ARQ22 and ARQ45 were cloned into plasmid pGEX-6P-1 (Addgene, Cambridge, MA, USA). The following fragments were cloned: AR(90-270), ARQ22(32-270) and ARQ45(32-293). Each of these fragments were cloned with either the wild-type KELCKAVSVSM(237-247) motif or the KELSKAVSVSM motif with a mutated cysteine. The same six AR NTD sequences were cloned into the expression vector pET-GB1a. Following isolation of the GB1a fusion proteins in His-agarose beads, the GB1a tag was cleaved off by Tobacco etch virus (TEV) protease.

SUMO-fusion constructs: The KELCKAVSVSM sequence was first cloned into a pETHis1a SUMO expression vector. Using the expression as a PCR template, a PCR reaction was performed with a T7 forward primer, 5′-TAATACGACTCACTATAGGGGAATTGTG-3′ and a reverse primer, 5′GGATCCTCACATGGACACCGACACTGCCTTACACAACTCCTTTGGCGCAGATCCACCAAT CTGTTCCTGTGAGC-3′. The reverse primer coded for a Bam HI restriction site, the stop codon, the peptide sequence of the human AR KELCKAVSVSM sequence and the C-terminal part of the SUMO protein (excluding the EGFP). The reverse primer also coded for a three amino acids Ser-Ala-Pro linker that were inserted between the peptide and the SUMO tag. A Xba I restriction site located downstream of the T7 promoter in the expression vector and a Bam HI restriction site were used for the cloning to generate SUMO_SAPKELCKAVSVSM construct that was verified by DNA sequencing.

E. coli Rosetta™(DE3) competent cells were used as the host strain for protein expression. The cells were transformed with the construct and protein expression induced either in Luria broth (LB) or in minimal media (M9) containing $^{15}NH_4Cl$ (0.5 g) and ^{13}C uniformly labeled glucose (2 g) per liter of culture as the sole source of nitrogen and carbon, respectively for NMR analysis [15,16]. The cells were harvested in lysis buffer (50 mM Tris-HCl, pH 8.0; 150 mM NaCl; 10 mM imidazole; 2 mM β-mecaptoethanol; 0.2 % NP-40, 2.5 U/ml DNAse 1, 2.5 mu/ml RNase A and a tablet of EDTA-free protease inhibitor cocktail (Roche)) and six sonication steps of 1 min each were performed with a Branson digital sonicator. The total cell lysate was centrifuged at 36,000 rpm for 1 h at 4 °C and the soluble fraction filtered through a Minisart High Flow syringe filter (Sartorius Biotech) with a pore size of 0.20 µm. The supernatant was loaded onto a Ni-NTA agarose resin column, pre-equilibrated

with the lysis buffer for gravity-flow chromatography using Econo-Pac columns (Bio-rad). The resin-bound protein was washed successively with the lysis buffer, wash buffer 2 (the lysis buffer minus NP-40), wash buffer 3 (wash buffer 2 plus 1 M NaCl), wash buffer 4 (wash buffer 2 plus 20 mM imidazole) and finally eluted with the wash buffer 2 containing 330 mM imidazole and 10 % glycerol.

4.2 Size exclusion chromatography analysis of SUMO-peptide fusion

The affinity purified SUMO-SAPKELCKAV fusion construct were concentrated and analyzed by size exclusion chromatography by injecting the samples onto a HiLoad 16/60 Superdex 75 prep grade column (GE healthcare), pre-equilibrated with 20 mM sodium phosphate buffer (pH 6.5), 150 mM NaCl with or without 2 mM DTT.

4.3 NMR experiments and formation of amyloid fibrils of KELCKAV peptides

The KELCKAV peptide in the SUMO construct was cleaved from the SUMO tag by incubating the fusion protein with a SUMO protease produced "in house" in a ratio of 1:100 at 30 °C for 1 hr. The cleaved peptide was then purified by reverse-phase high pressure liquid chromatography (RP-HPLC) using a preparative scale C18 column (Waters: PrePak cartridge, 21 x 250 mm, 300 A, 5 μM) with an acetonitrile gradient ranging from 10 % to 70 % in 0.1 % trifluoracetic (TFA). The peptide fractions were pooled together, lyophilized and either used immediately or stored at -20°C for later use. All NMR measurements were recorded on a 700 MHz Bruker Avance III HD spectrometer equipped with a Z gradient triple resonance cryogenic probe. Resonance assignments of the RP-HPLC purified KELCKAVSVSM peptides were obtained using standard homonuclear proton spectra (TOCSY and NOESY), ^{1}H-^{15}N- and ^{1}H-^{13}C HSQC heteronuclear correlation spectra and HNCA triple resonance spectra recorded at 298 K [17]. Proton chemical shifts were referenced using the 2,2-dimethyl-2-silapentene-5-sulfonate (DSS) as external standard, while ^{15}N and ^{13}C chemical shifts were calibrated indirectly using the values of their magnetogyric ratios [18]. As a control, ^{1}H-^{15}N HSQC heteronuclear correlation spectra for the SUMO-peptide fusion were also recorded. All spectra were processed using Topspin 2.1 (Bruker) and analyzed using CcpNmr [19].

The formation of KELCKAVSVSM fibrils was performed as previously described [14. Peptide fractions from RP-HPLC were pooled and lyophilized to remove acetonitrile. TFA was then removed from the peptide samples by three rounds of acidification (2 mM HCl) and lyophilization as described by Andrushchenko et al. [20] to remove TFA. The peptide was then resuspended in 100 % D2O, the pH adjusted to 7.0 and 10% of dimethyl sulfoxide (DMSO) added to obtain a final volume of 150 μl at 660 μM peptide concentration. The kinetics of fibril formation were monitored by NMR at 298 K and the fibrils imaged by transmission electron microscopy.

4.4 Atomic force microscopy(AFM) measurements of ARNTD constructs

The affinity purified AR NTD proteins were incubated at 60 μM in 50 mM Tris-HCl, pH 8.0 for 18 h at 37 °C to initiate the aggregation process before spotting on mica for AFM measurements. The samples were measured using a Nanoscope Dimension ICON in tapping mode in air scan rate of 1 Hz.

Acknowledgments: We thank Pascal Eberling of the peptide synthesis platform for help with the RP-HPLC analysis, Luc Negroni and Frank Ruffenach of the IGBMC proteomics platform for help with the mass spectrometry experiments and analysis, Christine Ruhlmann for help with the TEM images. The authors also like to thank Claude Ling for the excellent technical assistance. This work was financially supported by the ANR program ANR-13-BSV5-0013 – ARIA.

Author Contributions: M-A.D., A.C.B.C., and B.K. conceived and designed the experiments; E.O., M.G., R.S., and M.S. performed the experiments; E.O. and M-A.D., A.C.B.C., and B.K. analyzed the data; M.S. contributed reagents/materials/analysis tools; E.O. A.C.B.C. and B.K. wrote the paper.

Conflicts of Interest: The authors declare no conflict of interest. The founding sponsors had no role in the design of the study; in the collection, analyses, or interpretation of data; in the writing of the manuscript, and in the decision to publish the results.

References

1. P.M. Matias, P. Donner, R. Coelho, M. Thomaz, C. Peixoto, S. Macedo, N. Otto, S. Joschko, P. Scholz, A. Wegg, S. Basler, M. Schafer, U. Egner, and M.A. Carrondo, Structural evidence for ligand specificity in the binding domain of the human androgen receptor. Implications for pathogenic gene mutations. The Journal of biological chemistry 275 (2000) 26164-71.
2. B. He, R.T. Gampe, Jr., A.J. Kole, A.T. Hnat, T.B. Stanley, G. An, E.L. Stewart, R.I. Kalman, J.T. Minges, and E.M. Wilson, Structural basis for androgen receptor interdomain and coactivator interactions suggests a transition in nuclear receptor activation function dominance. Molecular cell 16 (2004) 425-38.
3. P.L. Shaffer, A. Jivan, D.E. Dollins, F. Claessens, and D.T. Gewirth, Structural basis of androgen receptor binding to selective androgen response elements. Proceedings of the National Academy of Sciences of the United States of America 101 (2004) 4758-63.
4. D.N. Lavery, and I.J. McEwan, Structural characterization of the native NH2-terminal transactivation domain of the human androgen receptor: a collapsed disordered conformation underlies structural plasticity and protein-induced folding. Biochemistry 47 (2008) 3360-9.
5. G. Jenster, H.A. van der Korput, C. van Vroonhoven, T.H. van der Kwast, J. Trapman, and A.O. Brinkmann, Domains of the human androgen receptor involved in steroid binding, transcriptional activation, and subcellular localization. Molecular endocrinology (Baltimore, Md.) 5 (1991) 1396-404.
6. J.A. Simental, M. Sar, M.V. Lane, F.S. French, and E.M. Wilson, Transcriptional activation and nuclear targeting signals of the human androgen receptor. The Journal of biological chemistry 266 (1991) 510-8.
7. A.R. La Spada, E.M. Wilson, D.B. Lubahn, A.E. Harding, and K.H. Fischbeck, Androgen receptor gene mutations in {X}-linked spinal and bulbar muscular atrophy. Nature 352 (1991) 77-79.
8. R. Kumar, H. Atamna, M.N. Zakharov, S. Bhasin, S.H. Khan, and R. Jasuja, Role of the androgen receptor CAG repeat polymorphism in prostate cancer, and spinal and bulbar muscular atrophy. Life Sci 88 (2011) 565-71.
9. T. Jochum, M.E. Ritz, C. Schuster, S.F. Funderburk, K. Jehle, K. Schmitz, F. Brinkmann, M. Hirtz, D. Moss, and A.C. Cato, Toxic and non-toxic aggregates from the {SBMA} and normal forms of androgen receptor have distinct oligomeric structures. Biochimica et biophysica acta 1822 (2012) 1070-1078.
10. B. Eftekharzadeh, A. Piai, G. Chiesa, D. Mungianu, J. Garcia, R. Pierattelli, I.C. Felli, and X. Salvatella, Sequence Context Influences the Structure and Aggregation Behavior of a PolyQ Tract. Biophysical journal 110 (2016) 2361-6.
11. H.M. Saunders, and S.P. Bottomley, Multi-domain misfolding: understanding the aggregation pathway of polyglutamine proteins. Protein Eng Des Sel 22 (2009) 447-51.
12. L. Masino, G. Nicastro, R.P. Menon, F. Dal Piaz, L. Calder, and A. Pastore, Characterization of the structure and the amyloidogenic properties of the Josephin domain of the polyglutamine-containing protein ataxin-3. J Mol Biol 344 (2004) 1021-35.
13. C. de Chiara, R.P. Menon, F. Dal Piaz, L. Calder, and A. Pastore, Polyglutamine is not all: the functional role of the AXH domain in the ataxin-1 protein. J Mol Biol 354 (2005) 883-93.
14. J. Asencio-Hernandez, C. Ruhlmann, A. McEwen, P. Eberling, Y. Nomine, J. Ceraline, J.P. Starck, and M.A. Delsuc, Reversible amyloid fiber formation in the N terminus of androgen receptor. Chembiochem : a European journal of chemical biology 15 (2014) 2370-3.
15. D. Martinez-Zapien, M.A. Delsuc, G. Trave, R. Lutzing, C. Rochette-Egly, and B. Kieffer, Production and characterization of a retinoic acid receptor RARgamma construction encompassing the DNA binding domain and the disordered N-terminal proline rich domain. Protein expression and purification 95 (2014) 113-20.
16. S. Meyer, Y.H. Wang, P. Perez-Escriva, and B. Kieffer, Backbone 1H, 15N, 13C NMR assignment of the 518-627 fragment of the androgen receptor encompassing N-terminal and DNA binding domains. Biomolecular NMR assignments 10 (2016) 175-8.
17. A. Bax, and S. Grzesiek, Methodological Advances in Protein Nmr. Accounts Chem Res 26 (1993) 131-138.
18. D.S. Wishart, C.G. Bigam, J. Yao, F. Abildgaard, H.J. Dyson, E. Oldfield, J.L. Markley, and B.D. Sykes, 1H, 13C and 15N chemical shift referencing in biomolecular NMR. J Biomol NMR 6 (1995) 135-40.

19. W.F. Vranken, W. Boucher, T.J. Stevens, R.H. Fogh, A. Pajon, M. Llinas, E.L. Ulrich, J.L. Markley, J. Ionides, and E.D. Laue, The CCPN data model for NMR spectroscopy: development of a software pipeline. Proteins 59 (2005) 687-96.
20. V.V. Andrushchenko, H.J. Vogel, and E.J. Prenner, Optimization of the hydrochloric acid concentration used for trifluoroacetate removal from synthetic peptides. Journal of peptide science : an official publication of the European Peptide Society 13 (2007) 37-43.
21. T.R. Butt, S.C. Edavettal, J.P. Hall, and M.R. Mattern, SUMO fusion technology for difficult-to-express proteins. Protein expression and purification 43 (2005) 1-9.
22. J.P. Tam, Cui Rong Wu, C. R.,Liu, W., Zhang, J. W., Disulfide bond formation in peptides by dimethyl sulfoxide. Scope and applications. J. Am. Chem. Soc. 113 (1991) 6657-6662.
23. E.F. Kuiper, E.P. de Mattos, L.B. Jardim, H.H. Kampinga, and S. Bergink, Chaperones in Polyglutamine Aggregation: Beyond the Q-Stretch. Front Neurosci 11 (2017) 145.
24. S.L. Crick, K.M. Ruff, K. Garai, C. Frieden, and R.V. Pappu, Unmasking the roles of N- and C-terminal flanking sequences from exon 1 of huntingtin as modulators of polyglutamine aggregation. Proceedings of the National Academy of Sciences of the United States of America 110 (2013) 20075-80.
25. A.K. Thakur, M. Jayaraman, R. Mishra, M. Thakur, V.M. Chellgren, I.J. Byeon, D.H. Anjum, R. Kodali, T.P. Creamer, J.F. Conway, A.M. Gronenborn, and R. Wetzel, Polyglutamine disruption of the huntingtin exon 1 N terminus triggers a complex aggregation mechanism. Nat Struct Mol Biol 16 (2009) 380-9.
26. L. Masino, G. Nicastro, L. Calder, M. Vendruscolo, and A. Pastore, Functional interactions as a survival strategy against abnormal aggregation. FASEB J 25 (2011) 45-54.
27. C.J. Lupton, D.L. Steer, P.L. Wintrode, S.P. Bottomley, V.A. Hughes, and A.M. Ellisdon, Enhanced molecular mobility of ordinarily structured regions drives polyglutamine disease. The Journal of biological chemistry 290 (2015) 24190-200.